

## Physical and Functional Interactions between ELL2 and RB in the Suppression of Prostate Cancer Cell Proliferation, Migration, and Invasion<sup>1,2</sup>



Xiaonan Qiu<sup>\*,†</sup>, Laura E. Pascal<sup>†</sup>, Qiong Song<sup>†,‡</sup>,  
Yachen Zang<sup>†,‡,§</sup>, Junkui Ai<sup>†</sup>, Katherine J. O'Malley<sup>†</sup>,  
Joel B. Nelson<sup>†</sup> and Zhou Wang<sup>†,‡,§,¶</sup>

\*Tsinghua MD Program, School of Medicine, Tsinghua University, Beijing, China; <sup>†</sup>Department of Urology, University of Pittsburgh School of Medicine, Pittsburgh, PA, USA; <sup>‡</sup>Center for Translational Medicine, Guangxi Medical University, Nanning, Guangxi, China; <sup>§</sup>University of Pittsburgh Cancer Institute, University of Pittsburgh School of Medicine, Pittsburgh, PA, USA; <sup>¶</sup>Department of Pharmacology and Chemical Biology, and University of Pittsburgh School of Medicine, Pittsburgh, PA, USA; <sup>#</sup>Department of Urology, The Second Affiliate Hospital of Soochow University, Suzhou, China

### Abstract

Elongation factor, RNA polymerase II, 2 (ELL2) is expressed and regulated by androgens in the prostate. ELL2 and ELL-associated factor 2 (EAF2) form a stable complex, and their orthologs in *Caenorhabditis elegans* appear to be functionally similar. In *C. elegans*, the EAF2 ortholog eaf-1 was reported to interact with the retinoblastoma (RB) pathway to control development and fertility in worms. Because RB loss is frequent in prostate cancer, ELL2 interaction with RB might be important for prostate homeostasis. The present study explored physical and functional interaction of ELL2 with RB in prostate cancer. ELL2 expression in human prostate cancer specimens was detected using quantitative polymerase chain reaction coupled with laser capture microdissection. Co-immunoprecipitation coupled with deletion mutagenesis was used to determine ELL2 association with RB. Functional interaction between ELL2 and RB was tested using siRNA knockdown, BrdU incorporation, Transwell, and/or invasion assays in LNCaP, C4-2, and 22Rv1 prostate cancer cells. ELL2 expression was downregulated in high-Gleason score prostate cancer specimens. ELL2 could be bound and stabilized by RB, and this interaction was mediated through the N-terminus of ELL2 and the C-terminus of RB. Concurrent siRNA knockdown of ELL2 and RB enhanced cell proliferation, migration, and invasion as compared to knockdown of ELL2 or RB alone in prostate cancer cells. ELL2 and RB can interact physically and functionally to suppress prostate cancer progression.

*Neoplasia* (2017) 19, 207–215

### Introduction

Loss of the retinoblastoma tumor suppressor gene (RB) has been reported in primary prostate tumors [1], and simultaneous gene methylation and allelic deletion of RB are frequent in castration-resistant prostate cancer [2,3]. In one study, deletion of the RB locus was reported in approximately 5% of primary tumors of prostate cancer and was predominantly associated (30%–40%) with castration-resistant prostate cancer [4]. Inactivation of RB has been shown to enhance the expression of androgen receptor, and knockdown of RB in LNCaP cells reduced their sensitivity to androgen ablation [1]. Conditional deletion of RB in prostate epithelial cells resulted in the induction of focal hyperplasia and murine prostatic intraepithelial

Address all correspondence to: Zhou Wang.

E-mail: wangz2@upmc.edu

<sup>1</sup> Contributions: X. Q. designed and performed experiments, and wrote the manuscript. Q. S. generated data for Supplemental Figure S2. All authors reviewed and edited the manuscript.

<sup>2</sup> This work was supported in part by National Institutes of Health grants R01 CA120386, 1P50 CA180995, T32 DK007774, and 1R50 CA211242, and scholarships from the Chinese Scholarship Council (X.Q.) and Tippins Foundation (L.E.P.). This project used the UPCI Tissue and Research Pathology Services and was supported in part by National Cancer Institute award P30CA047904.

Received 28 September 2016; Revised 22 December 2016; Accepted 2 January 2017

© 2016 The Authors. Published by Elsevier Inc. on behalf of SOCIETY. This is an open access article under the CC BY-NC-ND license (<http://creativecommons.org/licenses/by-nc-nd/4.0/>).  
1476-5586

<http://dx.doi.org/10.1016/j.neo.2017.01.001>

neoplasia in mouse models [5,6]. Cumulatively, these studies indicate that loss of function of RB is an important step in prostate carcinogenesis. Although RB disruption is strongly associated with tumorigenesis, the mechanisms by which RB dysfunction promotes prostate cancer progression still remain incompletely understood. Elucidation of interactions of the RB with its binding partners could provide greater insights into its role in suppressing prostate carcinogenesis.

Elongation factor, RNA polymerase II, 2 (ELL2) is a homolog of ELL1, which was initially identified based on its gene fusion with mixed-lineage leukemia in acute myeloid leukemia and named eleven-nineteen lysine-rich leukemia [7–9]. Transcription elongation plays a key role in efficient gene regulation and is frequently deregulated during cancer development and progression [10]. A variety of transcription elongation factors are involved in transcription elongation regulation of various genes [11]. ELL2 is a component of the super elongation complex which is required for rapid transcriptional induction in the presence or absence of paused Pol II [8,10,12]. ELL-associated factor 2 (EAF2) is tightly associated with ELL proteins [8,13]. ELL family proteins enhance transcription elongation, whereas EAF family proteins can stimulate transcription elongation activity of ELL proteins [8,14]. Inactivation of ELL or EAF orthologs in *Caenorhabditis elegans* resulted in identical phenotypes, suggesting that ELL and EAF family proteins act together to regulate downstream cellular pathways [15]. ELL2 and EAF2 were reported as androgen-response genes in the prostate [16–19]. EAF2 was also shown to act as a tumor suppressor in the murine prostate [17]. More recently, we identified genetic interactions between the EAF2 ortholog in *C. elegans* and the retinoblastoma protein (RB) signaling pathway [20]. Thus, ELL2 may also suppress prostate cancer and interact with RB signaling. Here we examined the function of ELL2 and its interactions with RB in human prostate cancer cells. Our studies suggest that ELL2 interacts with RB and plays a potential tumor suppressive role in prostate cancer.

## Material and Methods

### Laser-Capture Microdissection and Quantitative Polymerase Chain Reaction (qPCR)

Human prostate cancer tissue specimens without any previous chemo-, radio-, or hormone therapy were obtained from the UPCI Tissue and Research Pathology Services. Use of these prostate tissues was approved by the University of Pittsburgh Institutional Review Board. Prostate cancer cells and adjacent normal glandular cells were isolated by laser-capture microdissection using a Leica LMD6000 Microsystems microscope (Wetzlar, Germany) equipped with an HV-D20P Hitachi (Tokyo, Japan) color camera and Leica Laser Microdissection V 6.3 imaging software (Wetzlar, Germany). Captured individual tissue specimens were lysed, and RNA isolation, reverse transcription, and real-time qPCR were performed using CellsDirect One-Step qRT-PCR Kit (Invitrogen, Carlsbad, CA).

**Table 1.** siRNA Sequences for RB and ELL2

siRB-1	UUUGAAUUGGAUAAUCGUUCUUCUUCUCUG
siRB-2	UUUGGAAGAGGAAACAAUCUGCUACAA
siELL2-1	AUUUACAAUCUGAGGAGGAUGUGAGAU
siELL2-2	CAGUAAUGUGCAAGGUGAAAUGCUU

Gene-specific primers and Taqman probes cross exon/exon junctions and were designed previously [21] (Table 1). Probes contained FAM fluorophore and TAMRA quencher. TBP was purchased from Applied Biosystems (Foster City, CA). Primer and probe combinations were optimized and validated previously [21]. Real-time PCR was performed on a Bio-Rad IQ5 (Bio-Rad Laboratories, Hercules, CA) or ABI Step-One Plus (Applied Biosystems, Foster City, CA). Real-time PCR data were analyzed by  $\Delta C_p$  (crossing point) method as  $R=2^{[C_p \text{ sample} - C_p \text{ control}]}$  [21] to generate the relative expression ratio ( $R$ ) of each target gene relative to GAPDH.

### Data Analysis Using c-BioPortal

The c-BioPortal for Cancer Genomics site (<http://cbiportal.org>) was used to determine the alteration frequency in ELL2 and RB1 in prostate cancer data sets. Data from the Prostate Adenocarcinoma (TCGA, Provisional) case set was used to generate an OncoPrint with individual genes represented as rows and individual patients indicated as columns.

### Cell Culture, Overexpression, and Knockdown

For cell culture, cell lines LNCaP, 22RV1, HEK 293 (ATCC), and C4-2 (kind gift from Leland K. Chung) were cultured in RPMI-1640 (10-040-CV, Corning cellgro) or Dulbecco's modified Eagle's medium (12-604F, Lonza) supplemented with 10% fetal bovine serum (FBS) (S11150, Atlanta Biologicals) and 5% antibiotics.

For overexpression experiments, HEK 293 cells were transiently transfected with indicated expression vector(s) using PolyJet *In Vitro* Transfection reagent (SL100688, SignaGen Laboratories) according to the manufacturer's instructions. Cells were harvested and prepared for subsequent experiments 48 hours after transfection. After 48 hours, the transfected cells were directly lysed and analyzed by Western blot. After blocking for 1 hour at room temperature in 5% milk in phosphate-buffered saline/0.1% Tween-20, Western membranes were blotted using appropriate antibodies, including anti-ELL2 antibody (A302-505A, Bethyl) and anti-RB antibody (554136, BD Biosciences).

For knockdown experiments, cells in six-well plates were transfected with control siRNA (sc-37007 Santa Cruz) or siRNAs targeting RB or ELL2 using DharmaFECT siRNA transfection reagent (T-2001-03, Dharmacon). The final concentration of siRNA was 50 nM in each well. The control siRNA was used to complement the amount in single-knockdown groups. Forty-eight hours or at indicated times after transfection, the cells were used for further experiments or harvested. All siRNAs used against RB or ELL2 are listed in Table 2 and ordered from IDT (Integrated DN Technologies, USA). Two different siRNAs were used for each gene to confirm that the impact of siRNAs was due to knockdown of specific gene(s) and not because of their potential off-target effects.

**Table 2.** TaqMan Primers and Probes for qPCR

Gene	Primer/Probe	Species
ELL2	Forward: TGACTGCATCCAGCAAACAT	Human
	Reverse: TCGTTTGTTCACACACTGTAA	
	Probe: 6FAMTCTCCAGCTCTGGAGCCTCCCATAMRA	
GAPDH	Forward: CATGTTTCGTTCATGGGTGTGA	Human
	Reverse: GGTGCTAAGCAGTTGGTGGT	
	Probe: 6FAMACAGCCTCAAGATCATCAGCAATGCCTCTAMRA	

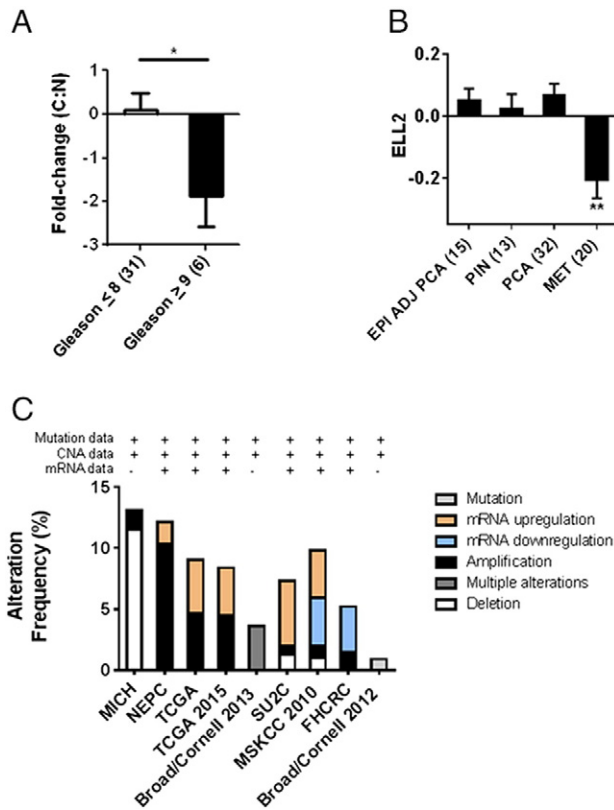


**Figure 1.** Expression of ELL2 in human prostate tumor specimens. (A) qPCR analysis of ELL2 expression in laser-capture microdissected human prostate tissue specimens from normal adjacent (N) and tumor cells (C) with Gleason score ≤ 8 compared to tumor specimens with Gleason score ≥ 9. Data are presented as ratio of expression C:N. (B) Microarray analysis of ELL2 mRNA expression in normal adjacent epithelial cells (EPI ADJ PCA), PIN lesions, prostate cancer (PCA), and metastases (MET) from Tomlins et al. [22]. Data are presented as the log2 normalized median of ratios (\**P* < .05, \*\**P* < .01). Number of patients for each group designated in parentheses. (C) ELL2 alteration in the top 14 publicly available genomic data sets from the cBioPortal for Cancer Genomics [23,24].

For Western blot analysis of proteins related to invasion, C4-2 cells were transfected with siControl, siELL2-1, and/or siRB-1 for 2 days. The cell lysates were then prepared and resolved on sodium dodecyl sulfate (SDS) polyacrylamide gel electrophoresis, and proteins were transferred to polyvinylidene difluoride membranes. The membranes were incubated overnight at 4°C with antibodies for Snail (3879, Cell Signaling Technology), Slug (9585, Cell Signaling Technology), E-cadherin (3195, Cell Signaling Technology), Vimentin (sc-73258, Santa Cruz Biotechnology), Twist (sc-15393, Santa Cruz Biotechnology), and GAPDH (sc-25778, Santa Cruz Biotechnology). GAPDH was used as loading control. Following secondary antibody incubation, immunoreactive proteins were visualized with an enhanced chemiluminescence detection system (Bio-Rad).

**Co-Immunoprecipitation**

For co-immunoprecipitation, HEK 293 cells in 10-cm culture plates were transiently transfected with 6 µg of the indicated plasmids, cultured for 48 hours after transfection, and lysed in lysis buffer (150

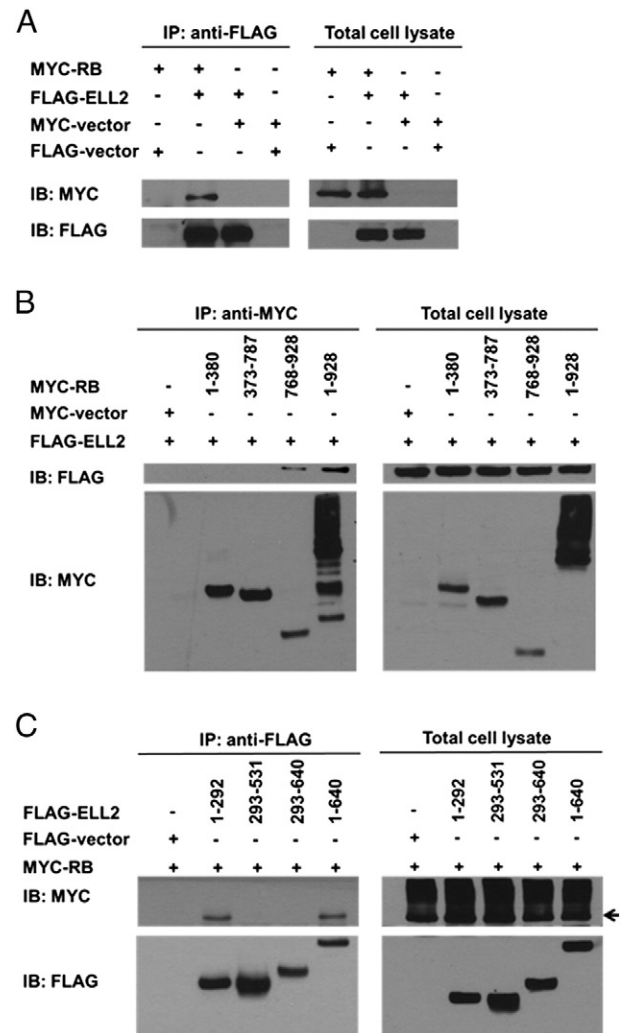


**Figure 2.** Co-immunoprecipitation of ELL2 with RB. (A) HEK 293 cells were transfected with flag-tagged wild-type ELL2 and myc-tagged wild-type RB, and proteins were co-immunoprecipitated. (B) HEK 293 cells were transfected with flag-tagged wild-type ELL2 and myc-tagged RB deletion mutants [amino acids (aa) 1-380, 373-787, 768-928]. (C) HEK 293 cells were transfected with myc-tagged wild-type RB and flag-tagged ELL2 deletion mutants (aa 1-292, 293-531, 293-640). The reactions were immunoblotted with Flag and Myc antibodies as indicated. Each blot is representative of three repeated experiments.

mM NaCl, 20 mM Tris-HCl, 1.5 mM MgCl<sub>2</sub>, 1% NP-40, 15% glycerol, 2 mM EDTA) with protease inhibitor cocktails (P8345-5ML, Sigma) at a dilution of 1:100. After precleaning cell lysates with protein A/G plus-agarose beads (sc-2003, Santa Cruz) for 1 hour and blocking anti-Flag (A2220-1ML, Sigma)/anti-Myc antibody-conjugated agarose beads (A7470-1ML, Sigma) with 2.5% albumin/bovine (94349-60-7, Acros organics) for 1 hour, cell lysates were added to anti-FLAG/anti-MYC antibody-conjugated agarose beads and rotated at 4°C for 1.5 hours. The beads were washed using lysis buffer four times. Immunoprecipitates and total cell lysates were boiled in SDS loading buffer for 10 minutes and then subjected to Western blot analysis using anti-Flag antibody (F1804-200UG, Sigma) and anti-MYC antibody (06-549, Sigma).

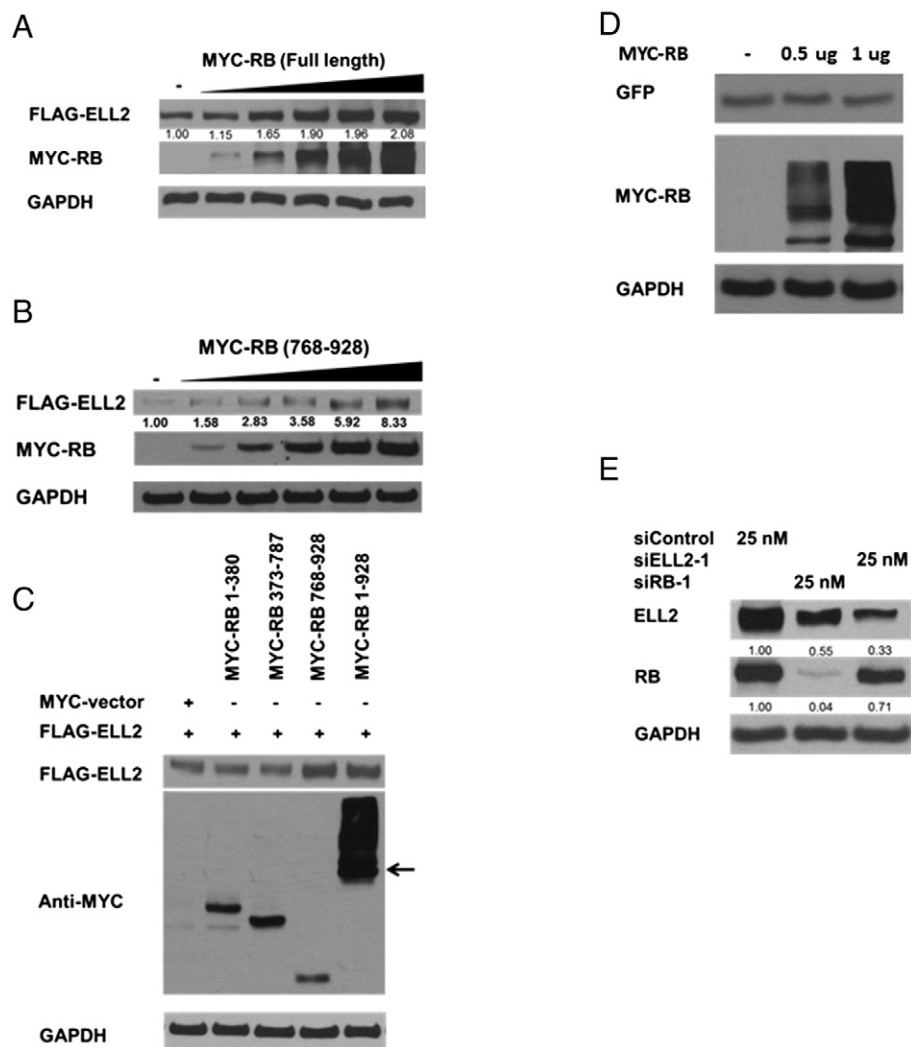


**Figure 3.** Stabilization of ELL2 by RB. (A) HEK 293 cells were transfected with 1  $\mu$ g flag-tagged wild-type ELL2 and increasing amounts of myc-tagged wild-type RB. (B) HEK 293 cells were transfected with 1  $\mu$ g flag-tagged wild-type ELL2 and increasing amounts of myc-tagged RB deletion mutant (aa 768-928). (C) HEK 293 cells were transfected with flag-tagged ELL2 plus wild-type RB or an myc-tagged RB deletion mutant (aa 1-380, 373-787, and 768-928). Arrow indicates unmodified myc-tagged RB protein. (D) HEK 293 cells were transfected with 1  $\mu$ g GFP expression vector and indicated amount of myc-RB expression vector. (E) Effect of siRNA knockdown of ELL2 on RB protein and vice versa in C4-2 cells. The cell lysates were immunoblotted with flag and myc antibody as indicated. Each blot is representative of three repeated experiments. GAPDH served as internal loading control.

### BrdU Assay

Cells seeded in 24-well plates were transfected with 50 nM of siRNA as indicated for 48 hours. The cells were subsequently cultured in the presence of 10  $\mu$ M BrdU (B5002-250MG, Sigma) for 2 hours (C4-2, 22RV1) or 16 hours (LNCaP) and then fixed by Carnoy's fixative (3:1 methanol:glacial acetic acid) for 20 minutes at  $-20^{\circ}\text{C}$ . After treatment with 2 M HCl, cells were washed with 0.1 M boric acid, then incubated with 3% hydrogen peroxide for 20 minutes at  $37^{\circ}\text{C}$ , followed by blocking with 10% goat serum for 1 hour at  $37^{\circ}\text{C}$ . Cells were then incubated with anti-BrdU antibody (B2521, Sigma) overnight at  $4^{\circ}\text{C}$  and CY3 labeled goat anti-mouse secondary antibody (A 10521, Life technologies) for 1 hour at  $37^{\circ}\text{C}$ . Nuclei were stained with 1  $\mu$ M SYTOX Green (S7020, Life technologies) for 15 minutes at room temperature.

Images were acquired using a fluorescence microscope (Nikon TE2000-U). C4-2 and LNCaP cells were counted using Photoshop CS5 counting tool (Adobe, San Jose, CA), whereas 22RV1 cells were

measured using ImageJ software (Wayne Rasband, National Institutes of Health, USA). The percentage of BrdU-positive cells was calculated using (BrdU-positive cell number/total cell number)\*100% for C4-2 and LNCaP cells or (BrdU-positive fluorescence area/SYTOX Green-positive area)\*100% for 22RV1 cells.

### Invasion Assay

Prostate cancer cells were transfected with siRNA at 50 nM each as indicated in a 6-well plate for 48 hours, then collected by trypsin treatment, and then embedded into Matrigel (354234, Matrigel matrix basement membrane, Corning) at a density of 125 cells/ $\mu$ l as 15- $\mu$ l pellets on the bottom of 12-well plates with 1 ml of RPMI-1640 with 10% FBS added. After incubation at  $37^{\circ}\text{C}$  for 48 hours (C4-2) or 72 hours (LNCaP), images were acquired using a Nikon Eclipse TS100 microscope using a 10 $\times$  objective. The cells were counted with the Photoshop CS5 counting tool (Adobe, San Jose, CA), and the percentage of invadopodia-positive cells was

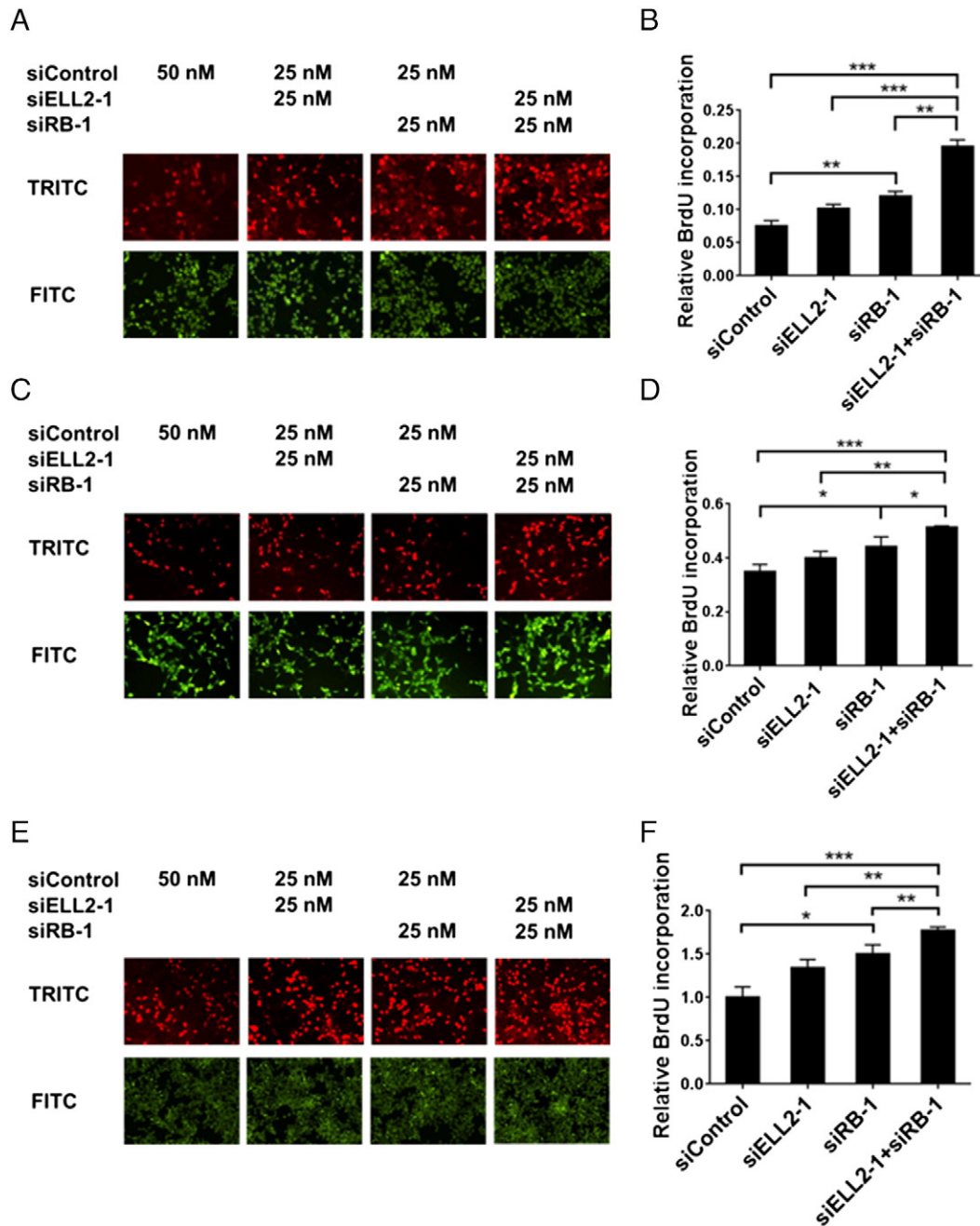


**Figure 4.** Effect of RB and/or ELL2 knockdown on prostate cancer cell proliferation. (A) BrdU incorporation in C4-2 cells transfected with nontargeted control (siCont) siRNA, targeted to ELL2 (siELL2-1), RB (siRB-1), or concurrent ELL2 and RB knockdown. Upper panel shows BrdU-positive nuclei (red), and lower panel shows nuclear staining with SYTOX Green (green). (B) Quantification of BrdU incorporation shown as mean percentage  $\pm$  SEM of BrdU-positive cells relative to the total number of cells. Results for A and B are representative of three individual experiments. (C) BrdU incorporation in LNCaP cells treated as in A. (D) Quantification of BrdU incorporation. (E) BrdU incorporation in 22RV1 cells treated as in A. (F) Quantification of BrdU incorporation (\* $P < .05$ , \*\* $P < .01$ , \*\*\* $P < .001$ ).

calculated using (invadopodia-positive cell number/total cell number)\*100%.

#### Migration Assay

Cell migration assay was performed in Transwell chambers (24-well, 8-mM pore size, Corning). C4-2 cells were transfected with siRNA at 50 nM each as indicated for 48 hours, collected by trypsin treatment, and then placed in the top chamber with 200  $\mu$ l of RPMI without FBS

(110,000 cells each chamber). As chemoattractant, 600  $\mu$ l of RPMI-1640 containing 20% FBS was placed in the bottom chamber. After 48 hours, nonmigrated cells on the top surface of the chamber membrane were removed by gentle scraping with cotton swabs. The migrated cells at the lower surface of chamber membranes were stained with 0.1% crystal violet (S25275B, Fisher Science Education). The number of migrated cells in five random high-power fields (10  $\times$  10) per membrane was counted under a microscope.

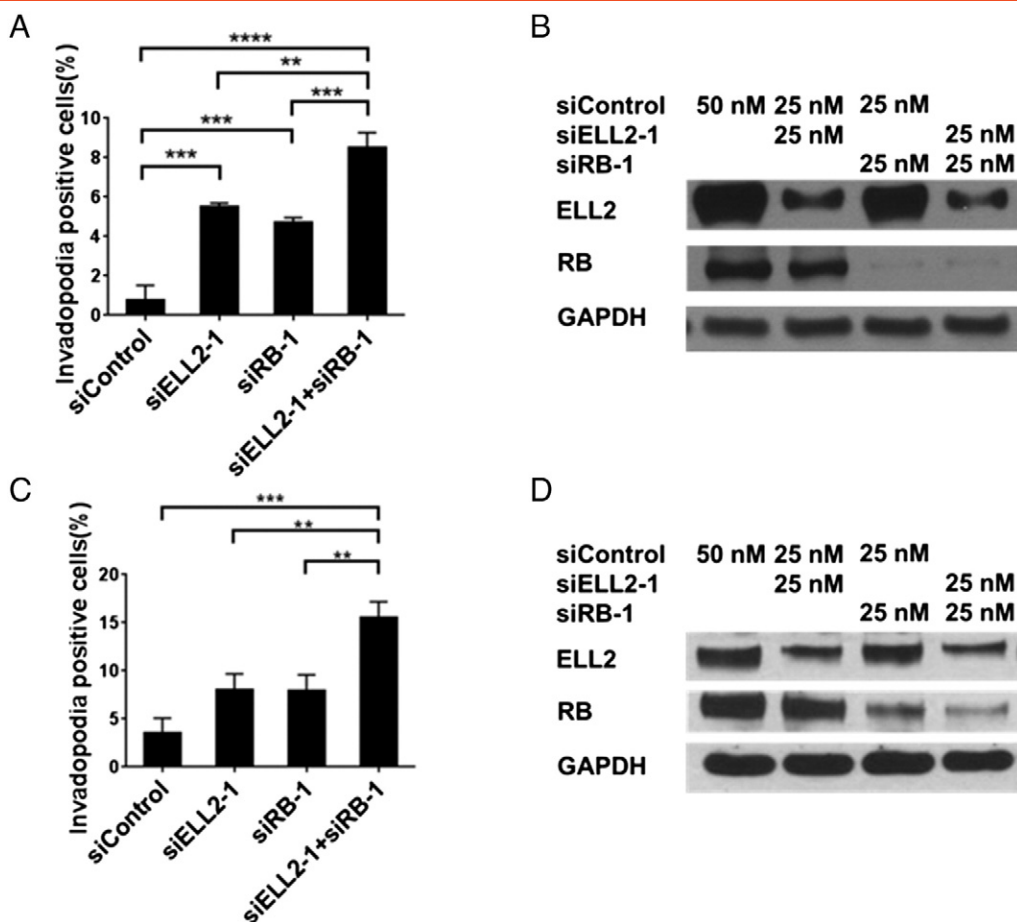


**Figure 5.** Effect of ELL2 and/or RB knockdown on prostate cancer cell invasion. (A) Quantification of invadopodia in C4-2 cells treated with siELL2, siRB-1, and concurrent siELL2-1 + siRB-1 for 48 hours. (B) Western blot analysis of ELL2 and RB protein from C4-2 cell lysates following siRNA knockdown as in A. (C) Quantification of invadopodia in LNCaP cells treated as in A. (D) Western blot analysis for LNCaP cells as in B. Invadopodia formation was determined by phase contrast microscopy 48 hours (for C4-2) or 72 hours (for LNCaP cells) after embedding cells in a 3D Matrigel matrix. Phase contrast microscopy images were analyzed for percent invadopodia-positive cells per optical field after ELL2, RB, and concurrent ELL2 and RB silencing with siRNA compared to siControl. GAPDH served as a loading control. Results are expressed as mean  $\pm$  SEM and are representative of three individual experiments. \* $P < .05$ , \*\* $P < .01$ , \*\*\* $P < .001$ .

### Statistical Analysis

Data are presented as mean  $\pm$  SEM. Statistical analyses were performed with Student's *t* test. \*, \*\*, and \*\*\* denote  $P < .05$ ,  $P < .01$ , and  $P < .001$ , respectively.

## Results

### Down-Regulation of ELL2 Gene Expression in Human Prostate Cancer Tissue Specimens

The expression of ELL2 was examined in human prostate tissue specimens by laser capture microdissection coupled with qPCR. ELL2 expression was not significantly different in tumors with Gleason score  $\leq 8$  compared to matched normal adjacent tissues. However, in tumors with Gleason score  $\geq 9$ , ELL2 expression levels were significantly decreased ( $P = .02$ ) (Figure 1A). In a study of prostate tumor specimens by Tomlins et al. [22], ELL2 expression was significantly decreased in metastases compared to primary prostate tumors, PIN lesions, and normal adjacent epithelial cells (Figure 1B). ELL2 loss was also examined in several large-scale genomics data sets available through the cBioPortal for Cancer Genomics [23,24]. Of the 11 prostate cancer genomics studies

available at the time of query, 9 data sets included ELL2 (Figure 1C). Interestingly, ELL2 alteration was most frequent in the Prostate Adenocarcinoma, Metastatic (Michigan, Nature 2012) data set (Figure 1C). This data set included 50 lethal heavily pretreated castration-resistant prostate cancers and 11 treatment-naive, high-grade localized prostate cancers [3]. These findings suggest that ELL2 loss is associated with advanced prostate cancer.

### Co-Immunoprecipitation of ELL2 with RB

Co-immunoprecipitation was used to determine the possibility of a physical interaction between ELL2 and RB in transiently transfected HEK 293 cells. MYC-RB was co-precipitated with FLAG-ELL2, suggesting that ELL2 and RB can be present in the same protein complex (Figure 2A). Attempts to co-immunoprecipitate endogenous ELL2 and RB proteins were unsuccessful, perhaps due to low expression levels of endogenous ELL2 and lack of high-quality anti-ELL2 antibodies suitable for co-immunoprecipitation. Subsequently, we used RB deletion mutants to explore which segment of RB was required for the interaction with ELL2. FLAG-ELL2 was co-precipitated by MYC-RB (aa768-928) or MYC-RB (full length)

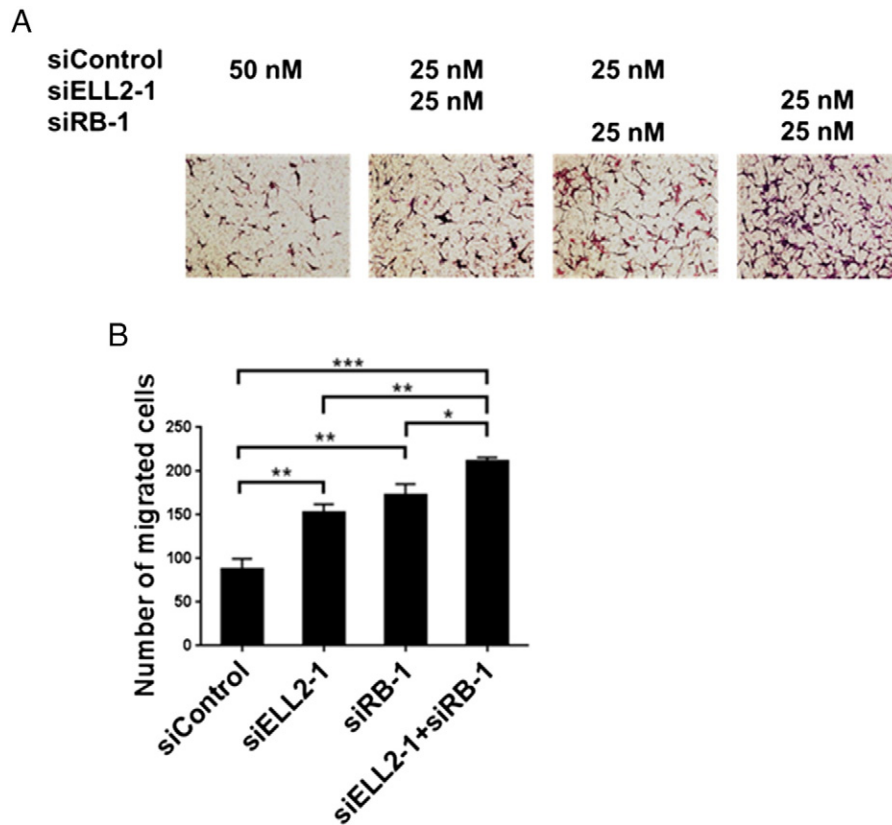


**Figure 6.** Effect of ELL2 and/or RB knockdown on C4-2 cell migration. (A) Haptotactic Transwell migration assay in C4-2 cells following siRNA knockdown of ELL2 and RB individually or concurrently after 48 hours with 10% FBS as chemoattractant. (B) Quantification of migrated cells. Results are expressed as mean  $\pm$  SEM and are representative of three individual experiments.

using anti-MYC antibody-conjugated agarose beads (Figure 2B). However, when MYC-RB (aa1-380) or MYC-RB (aa373-787) was used, no FLAG-ELL2 was co-precipitated (Figure 2B). These results suggested that the C-terminal domain of RB (aa768-928) was necessary for physical interaction of RB and ELL2. Truncated ELL2 mutants were used to identify which domain of ELL2 was required for interaction with RB. Myc-RB could be co-precipitated by Flag-ELL2 (aa1-292) and FLAG-ELL2 (full length) using anti-FLAG antibody conjugated agarose beads. In contrast, when FLAG-ELL2 (aa293-531) or FLAG-ELL2 (aa293-640) was used, there was no MYC-RB co-precipitated (Figure 2C). Thus, the N-terminal domain of ELL2 (aa1-292) was required for physical interaction of RB and ELL2.

#### The Effect of RB on ELL2 Protein Level

Because RB and ELL2 can interact with each other, we tested if RB could affect the protein level of ELL2. We transfected equal amount of FLAG-ELL2 plasmids with increasing amount of MYC-RB plasmids into HEK 293 cells, complemented with MYC empty vector. Western blot analysis showed increased protein levels of FLAG-ELL2 corresponding to increased levels of MYC-RB protein (Figure 3A), which suggested that RB could stabilize ELL2.

Because the C-terminal domain of RB (aa768-928) mediates physical interaction with ELL2, we tested whether it could stabilize ELL2. We transfected HEK 293 cells with increasing amount of MYC-RB (aa768-928) plasmids with equal amount of FLAG-ELL2 plasmids, complemented with MYC empty vector. FLAG-ELL2 protein level increased when increasing amount of MYC-RB

(aa768-928) was co-transfected (Figure 3B), indicating that the C-terminal of RB was critical for the stabilization of ELL2. To test whether other domains of RB could stabilize ELL2 protein, we transfected HEK 293 cells with equal amount of FLAG-ELL2 plasmid together with MYC-RB (full length), MYC-RB (aa1-380), MYC-RB (aa373-787), MYC-RB (aa768-928), or the empty MYC empty vector. FLAG-ELL2 protein level was enhanced when MYC-RB (aa768-928) or full-length MYC-RB vector was co-transfected but not when MYC-RB (aa1-380) or MYC-RB (aa373-787) was co-transfected. These observations suggested that the C-terminal of RB was necessary and sufficient for ELL2 stabilization (Figure 3C). We also tested if FLAG-ELL2 could stabilize MYC-RB in co-transfection experiments. However, the effect of FLAG-ELL2 co-transfection on MYC-RB protein level was marginal (data not shown).

As a control, we transfected HEK 293 cells with equal amount of GFP vector with different amounts of full-length MYC-RB complemented with MYC empty vector. No increase in GFP protein level was observed when it was co-transfected with different amounts of MYC-RB, which indicated that MYC-RB stabilization of FLAG-ELL2 was specific (Figure 3D).

To explore if endogenous RB could stabilize ELL2, we tested whether knockdown of endogenous RB can reduce the level of endogenous ELL2 protein in C4-2 cells. The result showed that RB knockdown could reduce the ELL2 protein level. We also tested the effect of ELL2 knockdown on RB level in C4-2 cells, and the result showed that ELL2 knockdown led to lower RB protein level (Figure 3E). These findings suggest that endogenous RB and ELL2 could stabilize each other.

### *The Effect of RB and/or ELL2 Knockdown on Prostate Cell Proliferation, Invasion, and Migration*

Because RB and ELL2 can be present in the same complex (Figure 2) and downregulation of ELL2 and RB expression was observed in prostate cancer specimens (Figure 1), we sought to determine whether RB and ELL2 downregulation individually or concurrently could impact proliferation, migration, and invasion of prostate cancer cells. We used BrdU assay to evaluate cell proliferation level after knockdown of RB and ELL2 separately and in combination in C4-2, LNCaP, and 22RV1 prostate cancer cell lines. Knockdown of RB enhanced BrdU incorporation in C4-2, LNCaP, and 22RV1 cell lines (Figure 4). All cell lines showed a slight increase of BrdU-positive cells in ELL2 knockdown group when compared to controls; however, the increase was not statistically significant (for C4-2,  $P = .0576$ ; for LNCaP,  $P = .0883$ ; and for 22RV1,  $P = .0724$ ). With depletion of both proteins, proliferation level was significantly enhanced when compared to either RB or ELL2 knockdown group (Figure 4). Knockdown of ELL2 or RB enhanced invasion of C4-2 and LNCaP when compared to the control groups, and combined knockdown of both proteins further enhanced invasion compared to single-knockdown groups (Figure 5). We also tested the migration ability of C4-2 cells after knockdown of RB and/or ELL2 protein. Although knockdown of RB or ELL2 individually could enhance migration, double knockdown significantly promoted cell migration compared to single-knockdown groups (Figure 6). Similar results were achieved in C4-2 cells treated with a second set of siRNA to control for potential off-target effects of siRNA (Supplemental Figure S1 in the online version at <http://dx.doi.org/10.1016/j.neo.2017.01.001>). Cumulatively, these results suggested that loss of both RB and ELL2 could profoundly stimulate prostate cancer proliferation, invasion, and migration.

Because ELL2 and RB knockdown enhanced invasion and migration of prostate cancer cells, we explored the effect of ELL2 and/or RB silencing on expression of a few genes related to invasion and metastasis, including Snail [25], E-cadherin [26], Vimentin [27], Twist [28], and Slug [29]. Knockdown of ELL2 and/or RB had no significant effect on the expression of these genes (Supplemental Figure S2 in the online version at <http://dx.doi.org/10.1016/j.neo.2017.01.001>).

### Discussion

This study presented evidence for ELL2 as a potential tumor suppressor in the prostate and its interaction with RB. ELL2 was downregulated in a subset of high-Gleason grade as well as in metastatic prostate cancer specimens (Figure 1). ELL2 co-immunoprecipitated with RB (Figures 2 and 3), and knockdown of both ELL2 and RB could significantly promote prostate cancer cell proliferation, migration, and invasion (Figures 4-6). These findings suggest that RB and ELL2 physically and functionally interact to suppress prostate cancer progression.

The co-IP of RB and ELL2 provides a potential mechanism for functional interactions between these two proteins. RB transfection enhanced the protein level of the co-transfected ELL2, whereas RB knockdown appeared to cause a reduction in the endogenous ELL2 protein in prostate cancer cells, suggesting that the binding of RB to ELL2 may enhance the protein stability. Similarly, ELL2 knockdown could reduce the protein level of endogenous RB. Thus, one potential mechanism for ELL2 and RB to work together synergistically could be their ability to enhance the protein levels of each other. In addition, binding of these two proteins to each other may enhance their recruitment of other binding partners.

The stabilization of transfected ELL2 by RB appears to be mediated through physical interactions between the two proteins. Deletion mutagenesis of RB coupled with co-IP showed that the C-terminal region of RB mediates the binding of RB to ELL2 through the N-terminal region of ELL2. Because ELL2 was stabilized by RB in transfected cells, we tested whether the C-terminal domain of RB was required for ELL2 stabilization. Because RB mutants lacking the C-terminal domain were unable to stabilize ELL2 whereas the C-terminal domain of RB was able to stabilize ELL2, the binding of RB to ELL2 appears to be necessary and sufficient for ELL2 stabilization.

ELL2 appears to be a potential tumor suppressor in the prostate because knockdown of ELL2 increased cell proliferation in multiple prostate cancer cell lines and ELL2 is down-regulated in high-Gleason grade and metastatic prostate cancer cells. These observations suggest that the role of ELL2 in prostate carcinogenesis is similar to EAF2, an ELL-associated factor and a potential tumor suppressor [13,17,18,30]. Our previous studies showed that inactivation of ELL2 and EAF2 orthologs caused similar phenotypes in the *C. elegans* model, suggesting that these two factors regulate similar signaling pathways [15]. Elucidating the mechanism of ELL2 action could provide new insights into the mechanism of EAF2 action and vice versa because they have similar functions.

Concurrent knockdown of RB and ELL2 enhanced proliferation, invasion, and migration in prostate cancer cell lines much more dramatically than the effect of RB or ELL2 knockdown individually (Figures 4-6). This observation suggests that RB and ELL2 can work together to suppress prostate carcinogenesis, and their combined loss should synergistically promote prostate cancer progression. The tumor suppressive activity of RB is stimulated by ELL2, and reciprocally, tumor suppression by ELL2 can be enhanced by RB. Thus, prostate tumor cells with concurrent loss of RB and ELL2 are likely more aggressive. Future studies will be needed to define the signaling pathways mediating synergistic interactions between ELL2 and RB and to evaluate whether concurrent loss of ELL2 and RB can be used to identify patients with high-risk prostate cancer.

Supplementary data to this article can be found online at <http://dx.doi.org/10.1016/j.neo.2017.01.001>.

### Acknowledgements

We are grateful to Lisa Gurski, Theosevia Demertzis, Marianne Notaro, Jianhua Zhou, and Aiyuan Zhang for technical support. This work was supported in part by National Institutes of Health grants R01 CA120386, 1P50 CA180995, T32 DK007774, and 1R50 CA211242, and scholarships from the Chinese Scholarship Council (X.Q.) and Tippins Foundation (L.E.P.). This project used the UPCI Tissue and Research Pathology Services and was supported in part by National Cancer Institute award P30CA047904.

### References

- [1] Sharma A, Yeow WS, Ertel A, Coleman I, Clegg N, Thangavel C, Morrissey C, Zhang X, Comstock CE, and Witkiewicz AK, et al (2010). The retinoblastoma tumor suppressor controls androgen signaling and human prostate cancer progression. *J Clin Invest* **120**(12), 4478–4492.
- [2] Whitaker LL, Su H, Baskaran R, Knudsen ES, and Wang JY (1998). Growth suppression by an E2F-binding-defective retinoblastoma protein (RB): contribution from the RB C pocket. *Mol Cell Biol* **18**(7), 4032–4042.

- [3] Grasso CS, Wu YM, Robinson DR, Cao X, Dhanasekaran SM, Khan AP, Quist MJ, Jing X, Lonigro RJ, and Brenner JC, et al (2012). The mutational landscape of lethal castration-resistant prostate cancer. *Nature* **487**(7406), 239–243.
- [4] Taylor BS, Schultz N, Hieronymus H, Gopalan A, Xiao Y, Carver BS, Arora VK, Kaushik P, Cerami E, and Reva B, et al (2010). Integrative genomic profiling of human prostate cancer. *Cancer Cell* **18**(1), 11–22.
- [5] Maddison LA, Sutherland BW, Barrios RJ, and Greenberg NM (2004). Conditional deletion of Rb causes early stage prostate cancer. *Cancer Res* **64**(17), 6018–6025.
- [6] Zhou Z, Flesken-Nikitin A, Corney DC, Wang W, Goodrich DW, Roy-Burman P, and Nikitin AY (2006). Synergy of p53 and Rb deficiency in a conditional mouse model for metastatic prostate cancer. *Cancer Res* **66**(16), 7889–7898.
- [7] Thirman MJ, Levitan DA, Kobayashi H, Simon MC, and Rowley JD (1994). Cloning of ELL, a gene that fuses to MLL in a t(11;19)(q23;p13.1) in acute myeloid leukemia. *Proc Natl Acad Sci U S A* **91**(25), 12110–12114.
- [8] Shilatifard A, Duan DR, Haque D, Florence C, Schubach WH, Conaway JW, and Conaway RC (1997). ELL2, a new member of an ELL family of RNA polymerase II elongation factors. *Proc Natl Acad Sci U S A* **94**(8), 3639–3643.
- [9] Shilatifard A, Lane WS, Jackson KW, Conaway RC, and Conaway JW (1996). An RNA polymerase II elongation factor encoded by the human ELL gene. *Science* **271**(5257), 1873–1876.
- [10] Luo Z, Lin C, and Shilatifard A (2012). The super elongation complex (SEC) family in transcriptional control. *Nat Rev Mol Cell Biol* **13**(9), 543–547.
- [11] Sims III RJ, Belotserkovskaya R, and Reinberg D (2004). Elongation by RNA polymerase II: the short and long of it. *Genes Dev* **18**(20), 2437–2468.
- [12] He N, Liu M, Hsu J, Xue Y, Chou S, Burlingame A, Krogan NJ, Alber T, and Zhou Q (2010). HIV-1 Tat and host AFF4 recruit two transcription elongation factors into a bifunctional complex for coordinated activation of HIV-1 transcription. *Mol Cell* **38**(3), 428–438.
- [13] Simone F, Luo RT, Polak PE, Kaberlein JJ, and Thirman MJ (2003). ELL-associated factor 2 (EAF2), a functional homolog of EAF1 with alternative ELL binding properties. *Blood* **101**(6), 2355–2362.
- [14] Kong SE, Banks CA, Shilatifard A, Conaway JW, and Conaway RC (2005). ELL-associated factors 1 and 2 are positive regulators of RNA polymerase II elongation factor ELL. *Proc Natl Acad Sci U S A* **102**(29), 10094–10098.
- [15] Cai L, Phong BL, Fisher AL, and Wang Z (2011). Regulation of fertility, survival, and cuticle collagen function by the *Caenorhabditis elegans* eaf-1 and ell-1 genes. *J Biol Chem* **286**(41), 35915–35921.
- [16] Wang Z, Tufts R, Haleem R, and Cai X (1997). Genes regulated by androgen in the rat ventral prostate. *Proc Natl Acad Sci U S A* **94**, 12999–13004.
- [17] Xiao W, Zhang Q, Habermacher G, Yang X, Zhang AY, Cai X, Hahn J, Liu J, Pins M, and Doglio L, et al (2008). U19/Eaf2 knockout causes lung adenocarcinoma, B-cell lymphoma, hepatocellular carcinoma and prostatic intraepithelial neoplasia. *Oncogene* **27**(11), 1536–1544.
- [18] Xiao W, Zhang Q, Jiang F, Pins M, Kozlowski JM, and Wang Z (2003). Suppression of prostate tumor growth by U19, a novel testosterone-regulated apoptosis inducer. *Cancer Res* **63**(15), 4698–4704.
- [19] Bolton EC, So AY, Chaivorapol C, Haqq CM, Li H, and Yamamoto KR (2007). Cell- and gene-specific regulation of primary target genes by the androgen receptor. *Genes Dev* **21**(16), 2005–2017.
- [20] Cai L, Wang D, Fisher AL, and Wang Z (2014). Identification of a genetic interaction between the tumor suppressor EAF2 and the retinoblastoma protein (Rb) signaling pathway in *C. elegans* and prostate cancer cells. *Biochem Biophys Res Commun* **447**(2), 292–298.
- [21] O'Malley KJ, Dhir R, Nelson JB, Bost J, Lin Y, and Wang Z (2009). The expression of androgen-responsive genes is up-regulated in the epithelia of benign prostatic hyperplasia. *Prostate* **69**(16), 1716–1723.
- [22] Tomlins SA, Mehra R, Rhodes DR, Cao X, Wang L, Dhanasekaran SM, Kalyana-Sundaram S, Wei JT, Rubin MA, and Pienta KJ, et al (2007). Integrative molecular concept modeling of prostate cancer progression. *Nat Genet* **39**(1), 41–51.
- [23] Gao JJ, Aksoy BA, Dogrusoz U, Dresdner G, Gross B, Sumer SO, Sun YC, Jacobsen A, Sinha R, and Larsson E, et al (2013). Integrative analysis of complex cancer genomics and clinical profiles using the cBioPortal. *Sci Signal* **6**(269).
- [24] Cerami E, Gao J, Dogrusoz U, Gross BE, Sumer SO, and Aksoy BA (2012). The cBio cancer genomics portal: an open platform for exploring multidimensional cancer genomics data (vol 2, pg 401, 2012). *Cancer Discov* **2**(10), 960.
- [25] Barrallo-Gimeno A and Nieto MA (2005). The Snail genes as inducers of cell movement and survival: implications in development and cancer. *Development* **132**(14), 3151–3161.
- [26] Wheelock MJ and Johnson KR (2003). Cadherins as modulators of cellular phenotype. *Annu Rev Cell Dev Biol* **19**, 207–235.
- [27] Nieminen M, Henttinen T, Merinen M, Marttila-Ichihara F, Eriksson JE, and Jalkanen S (2006). Vimentin function in lymphocyte adhesion and transcellular migration. *Nat Cell Biol* **8**(2), 156–162.
- [28] Yang J, Mani SA, Donaher JL, Ramaswamy S, Itzykson RA, Come C, Savagner P, Gitelman I, Richardson A, and Weinberg RA (2004). Twist, a master regulator of morphogenesis, plays an essential role in tumor metastasis. *Cell* **117**(7), 927–939.
- [29] Castro Alves C, Rosivatz E, Schott C, Hollweck R, Becker I, Sarbia M, Carneiro F, and Becker KF (2007). Slug is overexpressed in gastric carcinomas and may act synergistically with SIP1 and Snail in the down-regulation of E-cadherin. *J Pathol* **211**(5), 507–515.
- [30] Ai J, Pascal LE, O'Malley KJ, Dar JA, Isharwal S, Qiao Z, Ren B, Rigatti LH, Dhir R, and Xiao W, et al (2013). Concomitant loss of EAF2/U19 and Pten synergistically promotes prostate carcinogenesis in the mouse model. *Oncogene*.